Maunula, T., Ahola, J., Salmi, T., Haario, H., Härkönen, M., Luoma, M. and Pohjola, V., Investigation of CO oxidation and NO reduction on three-way monolith catalysts with transient response techniques, Applied Catalysis B: Environmental, 12 (1997) 287-308.

ELSEVIER Applied Catalysis B: Environmental 12 (1997) 287–308

APPLIED CATALYSIS B: ENVIRONMENTAL

Investigation of CO oxidation and NO reduction on three-way monolith catalysts with transient response techniques

Teuvo Maunula [a,*], Juha Ahola [b], Tapio Salmi [c], Heikki Haario [d], Matti Härkönen [a], Marjo Luoma [a], Veikko J. Pohjola [b]

[a] *Kemira Metalkat Oy, Catalyst Research, POB 171, FIN-90101 Oulu, Finland*
[b] *University of Oulu, Dept. of Process Engineering, FIN-90570 Oulu, Finland*
[c] *Åbo Akademi, Dept. of Chemical Engineering, FIN-20500 Turku, Finland*
[d] *Dept. of Mathematics, Univ. of Helsinki, FIN-00100 Helsinki, Finland*

Received 31 March 1996; revised 19 July 1996; accepted 20 August 1996

Abstract

The kinetics of CO oxidation and NO reduction reactions over alumina and alumina–ceria supported Pt, Rh and bimetallic Pt/Rh catalysts coated on metallic monoliths were investigated using the step response technique at atmospheric pressure and at temperatures 30–350°C. The feed step change experiments from an inert flow to a flow of a reagent (O_2, CO, NO and H_2) showed that the ceria promoted catalysts had higher adsorption capacities, higher reaction rates and promoting effects by preventing the inhibitory effects of reactants, than the alumina supported noble metal catalysts. The effect of ceria was explained with adsorbate spillover from the noble metal sites to ceria. The step change experiments CO/O_2 and O_2/CO also revealed the enhancing effect of ceria. The step change experiments NO/H_2 and H_2/NO gave nitrogen as a main reduction product and N_2O as a by-product. Preadsorption of NO on the catalyst surface decreased the catalyst activity in the reduction of NO with H_2. The CO oxidation transients were modeled with a mechanism which consisted of CO and O_2 adsorption and a surface reaction step. The NO reduction experiments with H_2 revealed the role of N_2O as a surface intermediate in the formation of N_2. The formation of N–N bonding was assumed to take place prior to, partly prior to or totally following to the N–O bond breakage. High NO coverage favors N_2O formation. Pt was shown to be more efficient than Rh for NO reduction by H_2.

Keywords: Carbon monoxide oxidation; Nitric oxide reduction; Three-way catalysts; Platinum; Rhodium

* Corresponding author.

PII S0926-3373(96)00084-7

1. Introduction

Simultaneous oxidation of carbon monoxide and hydrocarbons and reduction of nitrogen oxides (NO_x) are the most important reactions in automobile exhaust catalysis. The limiting factors of the process are the low conversion of CO and hydrocarbons in reducing conditions and the low conversion of NO_x in oxidizing conditions [1]. The significant reductants for NO reduction are CO, as well as hydrogen formed from hydrocarbons and through the water–gas shift reaction [2]. Thus a good exhaust catalyst should work within a large range of air-to-fuel (A/F) ratios, where the composition perturbation caused by feedback from the λ-sensor has frequencies about 0.5–4 Hz [3] and slow oscillations are due to the acceleration and deceleration phases during driving conditions [4]. The exhaust catalysts typically consist of noble metals (Pt, Rh, Pd) on a support material, such as alumina (Al_2O_3). The working range of the catalyst can be improved by addition of cerium oxide (CeO_2–Ce_2O_3, ceria) into the support material. The effect of ceria is based on its oxygen storage and transport properties: oxygen can be overspilt from the noble metal to ceria in oxidizing conditions and transferred back from ceria to the noble metals in reducing conditions [1,5].

For the design of catalytic converters for exhaust gases knowledge of the oxidation and reduction reaction kinetics is of considerable importance. Steady state measurements of the kinetics provide information of the overall performance of a catalytic converter, but these kinds of experiments are insufficient for the prediction of the catalyst performance in transient conditions. Furthermore, steady state measurements do not give unequivocal information of the underlying surface reaction mechanisms: typically several mechanisms lead to rate equations, which can equally well be fitted to experimental data.

Transient experimental techniques have turned out to be a powerful tool in the investigation of catalytic reaction mechanisms [6]. In transient conditions, the surface reactions in a catalytic cycle proceed at different rates. Thus, the measurement of the concentrations of reacting species in transient conditions gives direct information on the surface processes. Several transient techniques are available, for example, step response [7,8], pulse [6], cycling feeds [9], isotope and nonisothermal experiments, such as temperature programmed desorption (TPD), reduction (TPR), oxidation (TPO) and surface reaction (TPSR) [10,11]. The simple step response experiment, where the feeds of the reacting compounds are suddenly changed is the basic transient technique [6]. Extensive simulation studies have been published concerning the interpretation of step responses, i.e., deduction of surface reaction mechanisms from the forms of the response curves [7,12].

The endeavor of the present work is to elucidate the surface reaction mechanisms in automobile exhaust catalysis by studying some model reactions

with the step response technique. The model reactions chosen for this investigation were the oxidation of CO,

$$2\,CO + O_2 \rightarrow 2\,CO_2 \quad (1)$$

and the reduction of NO with H_2, which leads to the formation of N_2 as a main product and N_2O or NH_3 as by-products,

$$2\,NO + 2H_2 \rightarrow N_2 + 2\,H_2O \quad (2)$$

$$2\,NO + H_2 \rightarrow N_2O + H_2O \quad (3)$$

$$2\,NO + 5\,H_2 \rightarrow NH_3 + 2\,H_2O \quad (4)$$

The catalysts consisted of Al_2O_3 and CeO_2 supported Pt and Rh fixed on a metallic monolith.

2. Experimental

2.1. Catalysts

Five principal types of catalysts were used: Pt/Al_2O_3, Rh/Al_2O_3, Pt/Al_2O_3–CeO_2, Rh/Al_2O_3–CeO_2, Pt–Rh/Al_2O_3–CeO_2. The support material contents of the catalyst samples were usually about 40 g/m^2, but the support contents were varied in some of the samples. The catalyst samples were combinations of flat and corrugated metal foils (monoliths), which were coated with the support (γ-Al_2O_3 or γ-Al_2O_3–CeO_2) on which the noble metals were impregnated in aqueous solutions. $Pt(NH_3)_4Cl_2$ and $Rh(NO_3)_3$ were used as precursor salts. Some blank tests were made with the pure metal foil, as well as with the metal foil coated with the support material only. The physical properties of the catalysts-specific surface area (BET), pore volume and mean pore diameter were determined with nitrogen adsorption-desorption isotherms at -195°C and the dispersions of the noble metals were calculated from CO chemisorption isotherms at 25°C. Some characteristic data for the catalysts are given in Table 1.

2.2. Equipment

The experiments were carried out in a glass reactor especially designed to minimize the dead volumes in front of and behind the catalyst monolith. The catalyst monolith had a length of 28 mm and a diameter of approximately 8 mm. Two thermoelements were installed at the inlet and at the outlet of the monolith. The gases were fed into the reactor system through four-way valves to minimize pressure shocks which became visible as negative peaks at the moment of the feed exchange. All gas feeds were regulated with mass flow controllers. A scheme of the reactor system is shown in Fig. 1.

Table 1
The characterization of the catalyst samples

Catalyst	Support layer $g/m^2/\mu m$	Pt wt.%	Rh wt.%	Dispersion		BET m^2/g oxide	Pore volume cm^3/g	Mean pore diameter nm
				fresh %	treated %			
Pt/Al_2O_3	40/33	0.18	–	116	30	163	0.40	10
Rh/Al_2O_3	40/33	–	0.04	133	62	175	0.37	8
$Pt/Al_2O_3-CeO_2$	43/35	0.17	–	110	54	74	0.16	9
$Rh/Al_2O_3-CeO_2$	43/35	–	0.04	82	38	73	0.17	9
$Pt-Rh/Al_2O_3-CeO_2$	43/35	0.17	0.04	110	–	62	0.22	10
$Pt-Rh/Al_2O_3-CeO_2$	25/21	0.18	0.04	–	–	–	–	–
$Pt-Rh/Al_2O_3-CeO_2$	62/55	0.15	0.03	–	–	–	–	–

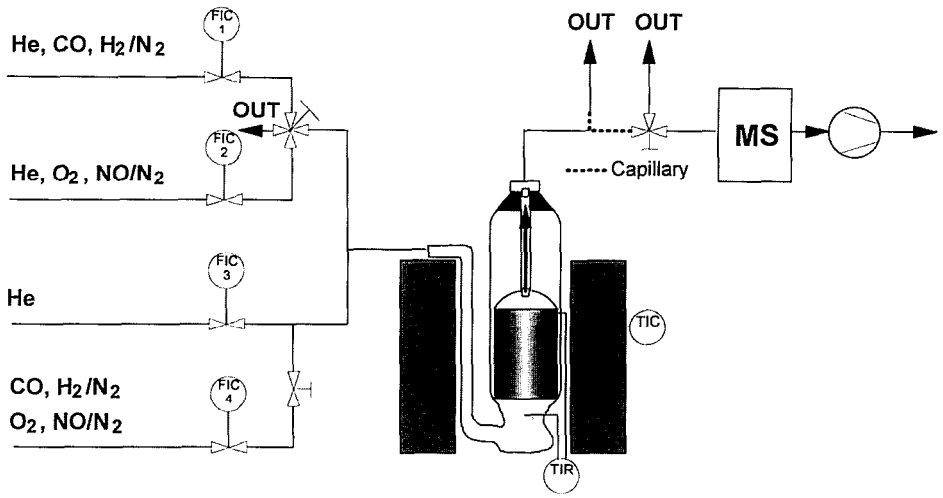

Fig. 1. The experimental equipment.

A split of the product flow was taken through a capillary into a quadrupole mass spectrometer (Balzers GAM 420) and the mass numbers of interest were monitored at 0.5 s intervals and stored in a computer. The sensitivity factors of the corresponding molecules were determined by calibration gas mixtures. The sensitivity factors were then used for the calculation of the gas concentrations from the intensities of the selected mass numbers.

2.3. Experimental procedures

Three principal types of step response experiments were performed: steps from an inert gas (He) to a reactant, steps from one reactant to another one and steps from a reactant flow to a flow of mixed reactants. The step response experiments were carried out at atmospheric pressure and in a temperature range of 30–350°C for all the catalysts as described in Table 2. It is however possible

Table 2
The step response experiments

Exp No.	Step change
1.1	He → 3.3% O_2 in He
1.2	He → 3.3% CO in He
1.3	3.3% CO ⇌ 3.3% O_2 in He
1.4	4.9% O_2 → 3.3% CO and 1.6% O_2 in He
1.5	4.6% CO → 2.9% CO and 1.7% O_2 in He
2.1	He → 1.0% NO in He and N_2
2.2	He → 1.0% H_2 in He and N_2
2.3	1.0% NO ⇌ 1.0% H_2 in He and N_2
2.4	2.0% H_2 → 1.0% NO and 1.0% H_2 in He and N_2
2.5	2.0% NO → 1.0% NO and 1.0% H_2 in He and N_2

Experimental temperatures: 1.1–1.5 at 30, 90, 150, 240 and 350°C; 2.1–2.5 at 30, 160, 200, 240 and 350°C.

to present precisely only the results containing the most pronounced information within this paper. The total volumetric flow was 300 cm^3/min (20°C, 1 atm). H_2 and NO were used as 10 vol-% mixtures in N_2; the other gases were used in research grade (> 99.997%). The background nitrogen used as a diluent in hydrogen and NO was subtracted from the total responses and nitrogen formed from NO was presented in results.

A virgin catalyst sample was always pretreated with the corresponding reactant mixture in a temperature programmed run, where the temperature was increased from 20°C to 350°C and the treatment was continued for 30 min in the elevated temperature, after which the sample was cooled down to room temperature under helium flow. The gas mixtures used in the pretreatments were: 3.3% CO + 2.0% O_2; 1.0% H_2 + 0.9% NO and 1.7% CO and 2.0% NO. Helium was used as a diluent.

For a binary gas mixture all experiments were carried out with the same catalyst sample. The experiments were performed starting from the lowest temperature then increasing the temperature to the next test. After completing the set of experiments the reactor was cooled down under He flow and the experiments of the next type were commenced.

For the transient adsorption experiments a different procedure was applied. The samples were reduced in a flow of 10% H_2/N_2 at 350°C for 15 min, after which the sample was cooled down to room temperature under He flow and the step response experiments were started. After the step response experiment the catalyst was regenerated under oxygen flow (3.3% O_2), until no oxidized products were detected in the product flow. The adsorption experiments were performed with the same catalyst sample in the following order: NO, H_2, O_2 and CO.

3. Results and discussion

3.1. Adsorption of O_2, CO, NO and H_2

The adsorption characteristics of Pt, Rh and Pt–Rh catalysts were studied with transient adsorption experiments using O_2, CO, NO and H_2 as adsorbates. The transient responses of the adsorbate molecules on a reduced sample were measured at 160–350°C after a step change from the inert (He) flow to the adsorbate flow. The step response obtained over an uncoated metal foil was used as a reference. Typical transient adsorption responses obtained for O_2, CO, NO and H_2 are presented in Fig. 2a–d, respectively. It is characteristic to all the adsorbate molecules that the response curve (the breakthrough curve) is virtually monotonic for the alumina supported Pt and Rh catalysts, whereas the breakthrough curve obtained for CeO_2 containing catalysts has two prominent parts. Generally the presence of Ce considerably enhances the adsorption capacity of the catalyst. For the adsorption of O_2 and H_2 no other molecules were detected

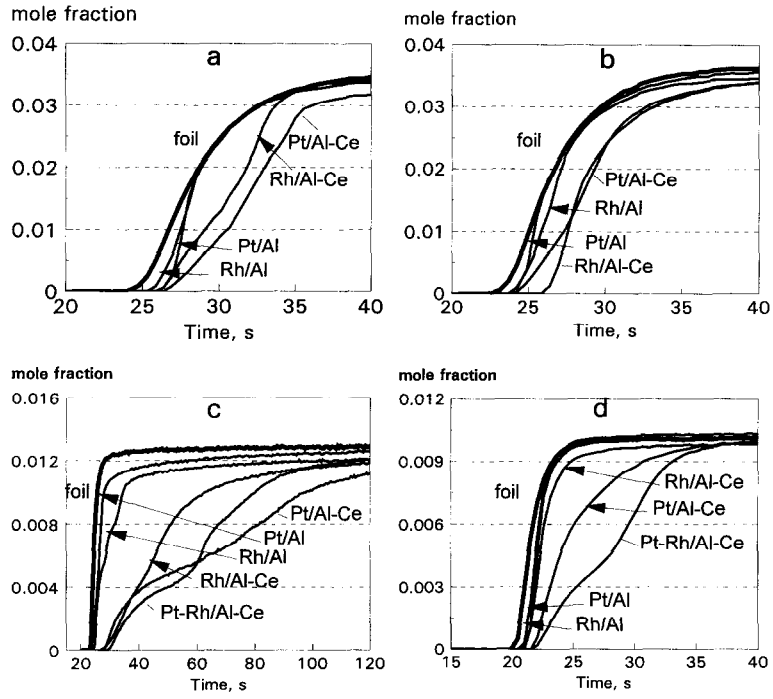

Fig. 2. Transient adsorption experiments: the response of O_2 (a) and CO (b) at 350°C, NO (c) and H_2 (d) at 160°C on Pt and Rh catalysts. The catalyst pretreatment with He.

in the mass spectra, whereas some CO_2 and some N_2O or N_2 were observed in the adsorption of CO and NO, respectively.

The specific amount of adsorbed substance ($\sigma_{i,ads}$) on the catalyst surface was calculated from the feed of adsorbate ($0i$), the outlet flow of the adsorbate (i) and the outlet flow of the product molecules (j):

$$\sigma_{i,ads} = \frac{n_0}{m}\int_0^{\infty}\left(x_{0i}(t) - x_i(t) - \frac{|v_i|}{|v_j|}x_j(t)\right)dt \tag{5}$$

where n_0 is the total inlet flow rate of substance, m is the mass of noble metals, x is molar fraction and v_i and v_j denote the stoichiometric coefficients of the reaction transforming the adsorbate. In the present case $v_i = v_j = 1$ was assumed for CO and $v_i = v_j = 2$ for NO adsorption. The adsorbed amounts were also calculated per catalyst material (washcoat + noble metals).

The capacities obtained for the different adsorbates and catalysts are summarized in Table 3. The results show that the ceria promoted catalysts have the highest adsorption capacity for all of the adsorbate molecules studied, whereas the unstabilized Pt and Rh catalysts had the lowest capacities. For CO adsorption the differences between the catalysts were minor. The calculated adsorption capacities per metal amounts at different temperatures revealed the effect of Ce

to also store adsorbates. Considerable amounts of CO_2 were formed only at the higher temperatures (350°C). The formation of CO_2 can principally progress via two routes: the catalyst surface is reduced, or CO is disproportioned to CO_2 and

Table 3
Adsorption capacities obtained from transient adsorption experiments

Oxygen adsorption			
Catalyst	Temperature	O_2 adsorption	
	°C	μmol/g cat	mmol/g NM
Pt/Al	150	1.1	0.6
	350	1.3	0.7
Rh/Al	150	2.2	5.8
	350	2.6	6.8
Pt/Al–Ce	150	18.9	11.4
	350	15.7	9.5
Rh/Al–Ce	150	9.4	25.4
	350	9.5	25.8

CO adsorption				
Catalyst	*T*°C	CO consumed μmol/g cat/ mmol/g NM	CO_2 produced μmol/g cat/ mmol/g NM	C_{surf} μmol/g cat/ mmol/g NM
Pt/Al	150	1.4/0.8	0.05/0.03	1.4/0.8
	350	2.9/1.7	1.3/0.7	1.6/0.9
Rh/Al	150	1.5/3.9	0.14/0.3	1.4/3.6
	350	3.1/8.1	1.3/3.4	1.8/4.8
Pt/Al–Ce	150	3.8/2.3	0	3.8/2.3
	350	14.0/8.3	8.6/5.2	5.3/3.2
Rh/Al–Ce	90	1.5/4.0	0	1.5/4.0
	150	1.3/3.6	0	1.3/3.6
	350	15.7/42.3	9.2/24.8	6.5/17.5

NO adsorption					
Catalyst	*T*°C	NO consumed μmol/g cat/ mmol/g NM	N_2 produced μmol/g cat/ mmol/g NM	N_2O produced μmol/g cat/ mmol/g NM	NO_{surf} μmol/g cat/ μmol/g NM
Pt/Al	30	10.9/6.3	–	1.4/0.8	8.1/4.6
	160	10.7/6.1	–	1.6/0.9	7.5/4.3
	350	19.9/11.4	0.2/0.1	5.3/3.0	8.9/5.1
Rh/Al	30	14.1/37.0	–	1.2/3.2	11.6/30.6
	160	11.2/29.4	–	1.2/3.2	8.7/23.0
	350	12.7/33.5	–	1.6/4.3	9.5/25.0
Pt/Al–Ce	30	53.1/32.0	4.9/3.0	7.3/4.4	28.6/17.2
	160	64.7/39.0	10.5/6.3	7.7/4.6	28.4/17.1
	350	60.3/36.3	17.5/10.5	6.5/3.9	12.3/7.4
Rh/Al–Ce	30	44.1/119	1.0/2.8	12.7/34.4	16.6/44.9
	160	45.1/122	4.0/10.7	9.3/25.1	18.4/50.1
	350	38.5/104	7.2/19.4	3.1/84.4	17.9/48.4
Pt–Rh/Al–Ce	30	46.0/22.3	6.8/3.3	8.4/4.1	15.6/7.6
	160	68.6/33.3	19.0/9.2	7.8/3.8	15.0/7.3
	350	62.6/30.4	20.4/9.9	4.5/2.2	12.7/6.

Table 3 (continued)

Hydrogen adsorption Catalyst	Temperature °C	H_2 adsorbed μmol/g cat	mmol/g NM
	160	0.8	0.4
Pt/Al	350	1.1	0.6
	30	1.2	3.2
Rh/Al	160	1.4	3.8
	350	0.9	2.4
	30	3.7	2.2
Pt/Al–Ce	160	5.9	3.6
	350	9.4	5.7
	160	2.4	6.4
Rh/Al–Ce	350	3.3	9.0
	30	4.8	2.3
Pt–Rh/Al–Ce	160	10.9	5.3
	350	10.4	5.0

NM = Noble metal.
i_{surf} = accumulation on surface.

carbon (C) on the surface. At higher temperatures the formation of CO_2 can be attributed to the water–gas shift reaction between CO and the hydroxyl groups of γ-alumina surface [13].

Adsorption of NO on the catalysts is a complicated matter, since the adsorption process is connected to the self-decomposition of NO. A typical example from the NO adsorption kinetics is shown in Fig. 3. NO is adsorbed on the surface at low temperatures (30°C) and it is partially converted to N_2 and N_2O (Table 3). The ceria promoted catalysts adsorbed more NO and formed more N_2 than the unpromoted Pt and Rh catalysts. In the beginning of the experiment all NO was adsorbed and no responses were detected at the outlet of the reactor. For the alumina supported catalysts and Rh/Al_2O_3–CeO_2 catalysts

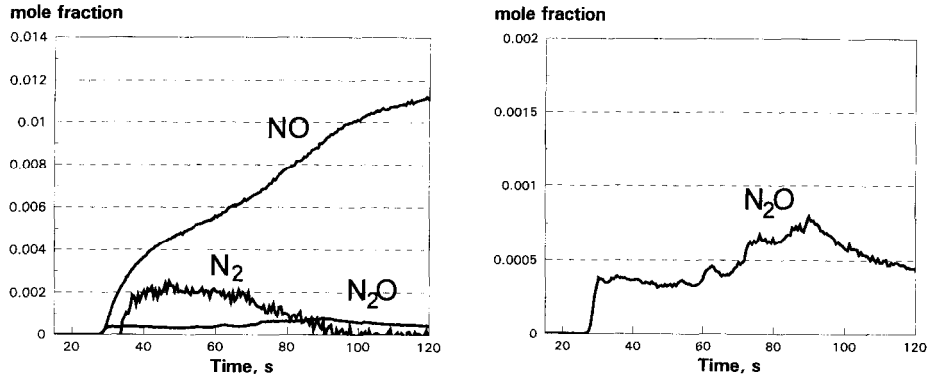

Fig. 3. The product distribution (N_2, N_2O) in the transient adsorption of NO on the Pt/Al_2O_3–CeO_2 catalyst at 160°C.

the responses were monotonic, and the NO concentration increased rapidly after the initial delay. The NO responses on the $Pt/Al_2O_3–CeO_2$ and on the $Pt–Rh/Al_2O_3–CeO_2$ catalysts possessed two inflexion points. This indicates a complicated adsorption mechanism, the adsorption probably taking place on different active sites. About 60–80% of the adsorbed NO reacted to N_2 and N_2O on reduced Ce containing catalysts. In spite of that there remained such a large amounts of NO on the surface that all of it could not be adsorbed on the noble metals. It is expected that a part of NO was adsorbed as nitrite and nitrate on the support material especially at lower temperatures [14]. The total amount of the consumed NO was near to the same on Pt/ and $Pt–Rh/Al_2O_3–CeO_2$ catalysts, but at lower temperatures instead of the reaction NO adsorption was relatively much higher on Pt catalyst. This showed the positive effect of Rh to dissociate and thus initiate the NO reaction on three-way catalysts.

The adsorption experiments with H_2 revealed that the adsorption affinity of H_2 is much less than that of NO. The catalyst containing ceria adsorbed more H_2 than the catalysts containing only Al_2O_3 as a support. The amounts of adsorbed H_2 were so small that all hydrogen can be adsorbed on the noble metals.

The adsorption studies revealed that all the compounds being studied in the reduction and oxidation reactions adsorb on the catalyst surfaces, but the ceria promoted catalysts had the highest adsorption capacity. The complex forms of the breakthrough curves observed for the ceria promoted catalysts indicate adsorption on different kinds of active sites as well as spillover on ceria. The differences on the rates at several temperatures showed that the rate of adsorption on ceria sites is slower than on noble metal sites. The adsorption on CeO_x crystals can be assumed to occur relatively slowly because of the larger particle sizes, higher concentrations and, in many cases, the poor ability of ceria to dissociate reactants without the assistance of noble metal. The interparticle diffusion of adsorbates from noble metal atoms proceeds slowly at the temperatures, where the kinetic limitations are negligible.

The surface area (BET) was not decreased by the experiments, but the dispersion degree was lower for reaction treated samples compared to fresh samples.

3.2. Oxidation of CO

Three kinds of CO oxidation feed exchange experiments were performed: oxidation of preadsorbed CO (CO/O_2) (a), oxidation of CO after preadsorption of oxygen (O_2/CO) (b) and a change of preadsorbed CO or O_2 to a mixture of CO and O_2 (c). Experiments (a) and (b) gave a pulse of CO_2, after which the reaction decayed. Examples of the CO/O_2 and O_2/CO exchange experiments performed on Pt catalysts are shown in Figs. 4 and 5, respectively.

The presence of preadsorbed CO on the surface had a considerable inhibitory

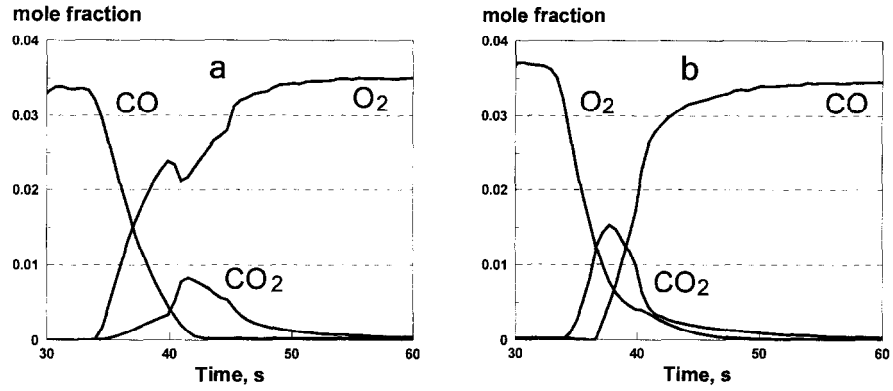

Fig. 4. CO/O_2 (a) and O_2 /CO (b) experiments on the Pt/Al_2O_3 catalyst at 150°C.

effect on the start-up of the adsorption of O_2 and thus on the whole oxidation process. The inhibitory effect of CO was most prominent for the Pt/Al catalyst, which has been presented at Fig. 4: the response of O_2 had a well-defined primary maximum followed by a minimum. This implies that O_2 fed into the reactor was blown out because the catalyst was not able to adsorb O_2 at the initial state. Later the catalyst is recovered, which resulted in the minimum in the O_2 response. This minimum also corresponds to the maximal production of CO_2. After this stage the CO coverage rapidly diminished, the production of CO_2 was deceased and the surface was covered by oxygen.

In the opposite type of step change experiment (O_2/CO) the production of CO_2 commenced immediately after the step change and the amount of produced CO_2 was larger than in the CO/O_2 exchange experiments. The results of the reaction experiments agree well with the adsorption experiments, which suggested that the CO adsorption capacities of the Pt and Rh catalysts would be higher than their O_2 adsorption capacity (Table 3). Because the moles of

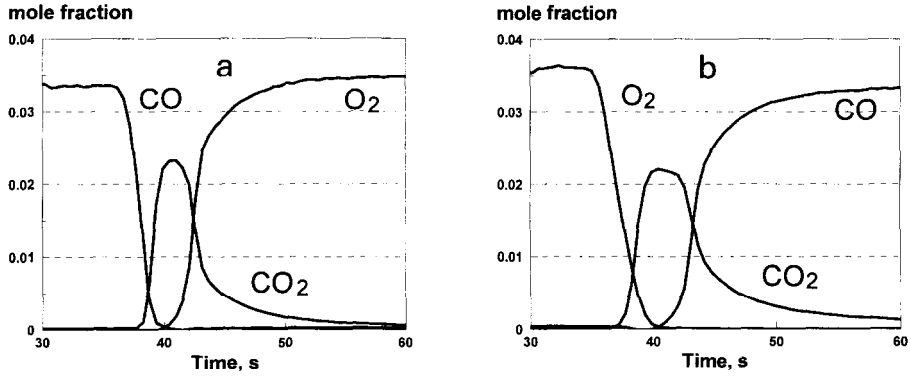

Fig. 5. CO/O_2 (a) and O_2 /CO (b) experiments on the Pt/Al_2O_3–CeO_2 catalyst at 150°C.

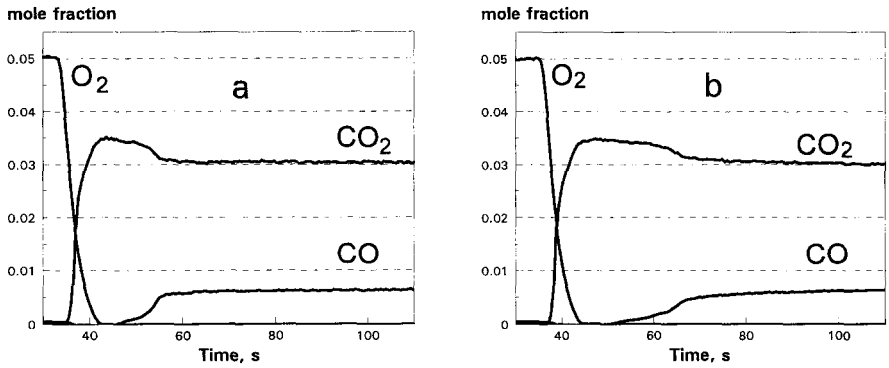

Fig. 6. O_2 / $(CO + O_2)$ experiments on the Rh/Al_2O_3–CeO_2 catalyst at 240°C (a) and 350°C (b).

dissociated oxygen on the surface are twofold compared to molecular oxygen in the gas flow, oxygen has a higher capacity to occupy the active sites more quickly than the same amount of CO in gas phase.

The presence of ceria considerably changed the reaction behavior of the catalyst (Fig. 5). The amount of CO_2 formed was higher than on alumina supported Pt and Rh catalysts as can be seen for Pt catalysts by comparison of Figs. 4 and 5. Furthermore, preadsorption of CO on the surface did not have such a deteriorating effect on the adsorption of O_2 and on the oxidation reaction: a CO_2 pulse was observed virtually immediately after the CO/O_2 exchange. The forms of the CO_2 pulses were similar for CO/O_2 and O_2/CO experiments (Fig. 5), but the amount of CO_2 produced was higher in the O_2/CO experiment.

The exchange experiments from O_2 to a reaction mixture (CO, O_2) always gave an overshooting response of CO_2 as can be seen from Fig. 6. The responses were principally similar for the unpromoted and the ceria promoted noble metal catalysts, but the maximum of the CO_2 response was broader for the ceria promoted catalyst. This observation indicates that there exists an optimal set of surface coverages of CO and dissociated O_2, giving the maximal CO_2 production rate. As shown by previous simulation studies [7,15] this kind of response is obtained for a Langmuir-Hinshelwood mechanism, where the surface reaction and the adsorption of the reagent are slow steps.

The transient exchange experiments on Pt and Rh catalysts indicate that the oxidation proceeds via a Langmuir-Hinshelwood mechanism on the metal sites (*). e.g.,

$$CO + {}^* \rightleftharpoons CO^* \tag{6}$$

$$O_2 + 2\,{}^* \rightleftharpoons 2\,O^* \tag{7}$$

$$CO^* + O^* \rightarrow CO_2 + 2\,{}^* \tag{8}$$

This mechanism proposed earlier by many authors [9,15] explains the time delays in the formation of the CO_2 pulses in the CO/O_2 and O_2/CO experi-

ments. The adsorption equilibria in the experiments are clearly shifted to the product sides of Eqs. (6) and (7). At lower temperatures vacant sites of * are few, but O_2 dissociation needs two adjacent free sites, where also the probabilities are very low. This explains the inhibitory effects of CO in the reaction. The adsorption capacity of CO was higher than that of O_2 on the Pt/Al catalyst, which leads to higher initial surface coverage of CO in the CO/O_2 exchange experiment than the initial surface coverage of O_2 in the O_2/CO experiment. This might explain the differences in the CO_2 pulses observed in the experiments (Fig. 4). At higher partial pressures an Eley-Rideal mechanism could also be possible ($CO + O^* \rightarrow CO_2^*$). Recently, it has been assumed that inactive Rh_2O_3 decreases the reaction rate in lean-rich switch. Pt catalysts are more active, because PtO_2 decomposes at a lower temperature range. On bimolecular Pt–Rh catalyst Pt maintains activity during the lean phase and Rh contributes to reaction in rich conditions.

For the ceria promoted catalysts the higher reaction rate is explained by oxygen spillover, which transfers oxygen from noble metals to ceria and provides new vacant sites for adsorption on the noble metal sites (*)

$$O^* + \# \rightleftharpoons {}^* + O\# \tag{9}$$

where # denotes a site on ceria. The totally oxidized surface denotes the oxidation state of CeO_2 and the totally reduced surface to $CeO_{1.5}$ in these conditions. The Al–Ce and Al carriers itself were detected to be inactive for CO oxidation at lower temperatures. This oxygen spillover was assumed to happen at the Pt–CeO_x interface, where all reducible surface oxygen atoms diffuse because of the concentration gradient. In lean conditions oxygen vacancies can diffuse in the opposite direction. This lead us to an assumption that on CeO_x containing catalysts the concentration of oxygen during lean conditions has higher phase effects on the total reaction activity than on Ce-free catalysts, as concluded also from the studies by Serre et al. [16].

This hypothesis of spillover is further supported by the high oxygen storage capacity of the ceria promoted catalysts (Table 3). Thus the oxygen breakthrough curves observed for ceria promoted catalysts can be explained by the oxygen adsorption and spillover step (8). This phenomenon was earlier explained by the solid state catalysis of noble metals to oxidize and reduct solid oxides, which requires extremely intimate contact between them [17,18]. Pt was supposed to decrease the Ce–O and C–O bond strength [13], but CO is not dissociated.

The first step of the reaction was earlier assumed to be between CO^* and O# [16] but because of low activity of Ce for this reaction, we prefer to propose that oxygen from the ceria interface moves before reaction to the Pt surface. Our earlier TPD studies on principally similar Al_2O_3 and Al_2O_3–CeO_2 supported catalysts showed that CeO_2 increases considerably the activation energies of CO and NO desorption [19]. During the CO/O_2 exchange experiment this also

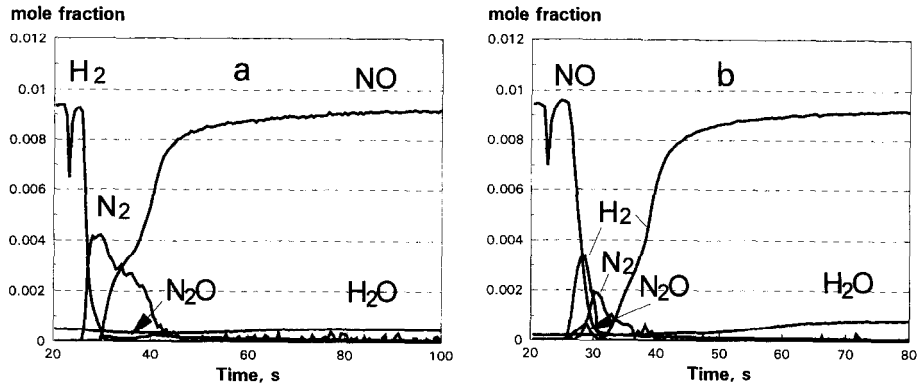

Fig. 7. H_2 /NO (a) and NO/H_2 (b) experiments on the Rh/Al_2O_3–CeO_2 catalyst at 240°C.

explains the enhancement of the reaction. CO/(CO + O_2) step was also used to check whether any mass transfer limitations exist. No mass transfer limitations because of pore diffusion were detected when Al–Ce washcoat thickness was varied between 21 and 55 μm.

3.3. Reduction of NO

The reduction kinetics of NO with H_2 was studied with four types of transient response experiments, with step changes from H_2 to NO, from NO to H_2, from H_2 to a mixture of H_2 and NO and from NO to a mixture of H_2 and NO. Some results from the NO/H_2 and H_2/NO exchange experiments over Rh/Al–Ce are depicted in Figs. 7–9. N_2 was the main product, but small amounts of N_2O were always released from the catalyst surface as a by-product. The amount of N_2 formed was clearly higher for the ceria promoted catalysts than for the unpromoted Pt and Rh catalysts.

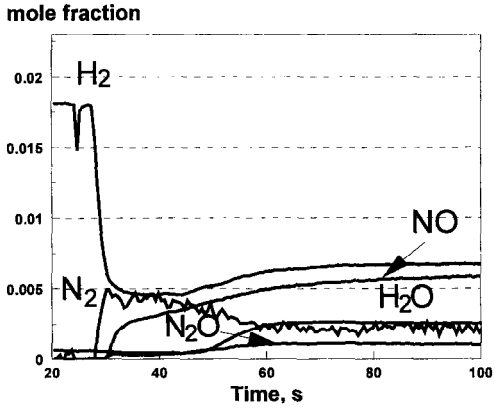

Fig. 8. H_2 / (H_2 + NO) experiments on the Rh/Al_2O_3–CeO_2 catalyst at 160°C.

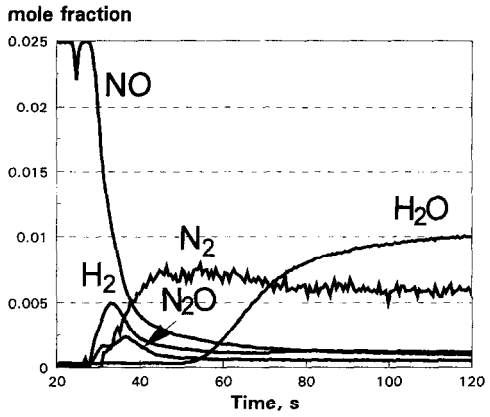

Fig. 9. NO/ (H_2 + NO) experiments on the Rh/Al_2O_3–CeO_2 catalyst at 240°C.

The amount of N_2 was clearly higher in the H_2/NO exchange experiments than in the NO/H_2 experiments. The amount of water could not be determined very precisely, but the analysis indicated that the amount of H_2O formed was much less in the H_2/NO experiments than in the NO/H_2 experiment. This incidates that after NO preadsorption surface is covered by oxygen or oxygen containing complexes, the amount of which is larger than the amount of hydrogen after hydrogen preadsorption. For the ceria promoted catalyst the amount of water was higher than for the alumina supported Pt and Rh catalysts. This indicates that, oxygen in ceria lattice is available for the reaction.

Preadsorption of NO had a deteriorating effect on the catalytic activity at lower temperatures (Fig. 7). The amount of released N_2 was minor and the adsorption of H_2 was inhibited by the presence of NO and its decomposition products on the surface. This can be seen from the primary maximum in the H_2 response (Fig. 7b): H_2 refuses the catalyst until some surface sites become vacant after N_2 desorption.

The H_2/(H_2 + NO) exchange experiments confirmed the observations made in the H_2/NO and NO/H_2 exchange experiments. A pulse of N_2 was observed and this maximum in the N_2 response corresponded to a minimum in the H_2 response (Fig. 8). The presence of NO on the surface inhibited hydrogen adsorption in such a way that the response of H_2 had a maximum at the initial stage after the step change (Fig. 9). After the increase of the H_2 adsorption N_2 commences to be released from the surface.

The response of H_2O was in all cases monotonically increasing (e.g., Fig. 9), but it had much slower dynamics than the responses of the gaseous molecules. Obviously the desorption rate of H_2O is slow and mass transfer limitations are present in the response of H_2O. The condensation of H_2O in the equipment could, however, not been completely excluded, so further speculation on the behavior of water is fruitless.

The interpretation of the step responses in the reduction of NO should principally give an indication of the adsorption state and the dissociation of NO, as well as of the role of N_2O as a reaction intermediate and the interaction of NO with hydrogen on the surface. The adsorption steps of NO and H_2 on the noble metal surface can be sketched as follows:

$$NO + {}^* \rightleftharpoons NO^* \tag{10}$$

$$H_2 + 2\,{}^* \rightleftharpoons 2\,H^* \tag{11}$$

The most important step for NO reduction to proceed is the formation of a N–N bond between adjacently adsorbed nitrogen species. The adsorbed NO molecules can form a surface complex, which dissociates to N_2O and oxygen or N_2 and oxygen

$$2\,NO^* \rightleftharpoons {}^*ON\ldots NO^* \tag{12}$$

$${}^*ON\ldots NO^* \rightleftharpoons N_2O^* + O^* \tag{13}$$

$${}^*ON\ldots NO^* \rightarrow N_2 + 2\,O^* \tag{14}$$

This mechanism scheme describes the fixation route of two nitrogen atoms into the same intermediate. This kind of intramolecular coupling of nitrosyls to form dinitrogen dioxide which rearranges to a *cis*-hyponitrite was proved to be thermodynamically possible but kinetically restricted when Fe was an active center [20]. The stability of the similar intermediate is plausible on noble metal surfaces. Adsorbed NO could also dissociate directly to nitrogen and oxygen, which gives a possible route for the nitrous oxide and nitrogen formation:

$$NO^* + {}^* \rightleftharpoons N^* + O^* \tag{15}$$

$$N^* + NO^* \rightleftharpoons N_2O^* + {}^* \tag{16}$$

$$2\,N^* \rightarrow N_2 + 2\,{}^* \tag{17}$$

In both mechanisms gas phase N_2O is formed through desorption and N_2 can also be formed from N_2O^*

$$N_2O^* \rightleftharpoons N_2O + {}^* \tag{18}$$

$$N_2O^* \rightarrow N_2 + O^* \tag{19}$$

N_2O^* is consumed by reaction associated dissociation or decomposition. On noble metal catalysts both alternatives are possible. As single reaction N_2O decomposition is negligible when $< 400°C$ and strongly inhibited by H_2 or CO [21], but in the case of N_2O^* formed by Eq. (16), N_2O can react to N_2 at lower temperatures. Both mechanisms give the same overall reaction, which makes it difficult to decide the true mechanism. The main question is whether two NO molecules break the N–O bond totally (via N), partly (via N_2O) or not at all (via ON...NO) prior to the N–N bond formation. NO reduction by dissociation has been proven by many studies [15,22], but the proposed ON...NO mechanism

can proceed straightly by (14) or it is reaction assisted. The reductants catching oxygen from ON...NO are efficient assistants for the nitrogen fixation. The ON...NO intermediate has been proposed to be attached to two adjacent sites, but more accurate surface studies are necessary to find out, whether adsorption on a single vacant site is possible (ON...NO*). All three mechanisms are principally potential, but the dominating path is dependent particularly on the catalyst composition, the reactant concentrations and the temperature. These steps lead to the consumption of vacant sites and to the accumulation of oxygen (O*) on the surface. For ceria promoted catalysts the accumulated oxygen can partially be spilt over to ceria according to Eq. (9), which regenerates vacant sites on the noble metal and thus explains the higher activity of these catalysts. Close to the light-off temperature range of three-way catalysts oxygen desorption is not probable [23], but it is necessary for oxygen to be consumed by reactions to regenerate active sites.

The role of N_2O in the reaction path is of crucial importance in the interpretation of the transient responses. Some N_2O was also formed at the steady state around 200°C and the response of N_2O was monotonically increasing. At lower temperatures the response of N_2O typically had two distinct maxima. The first one was detected at the same time as nitrogen formation initiated and the second one when the nitrogen formation was reaching the steady state rate in the mixture of NO and hydrogen. The nitrous oxide mechanism for the N_2 formation explains the detected second maxima and overshoots of N_2O responses in some step experiments which are more difficult to explain solely with the ON...NO mechanism. No NO_2 formation was detected in these experiments. Ammonia formation was possible during NO–H_2 reactions, but its response was not detectable, because of the overlap of NH_3 and OH (from water) at mass numbers 17. The subsequent NH_3–NO reaction may cause a dramatic increase in NO conversion [24]. Particularly at the beginning of H_2/NO exchange, NH_3 can be formed and later it reacts with NO which rapidly occupies the free active sites.

In the $H_2/(H_2 + NO)$ step Rh favored the formation of N_2O at 200°C (Fig. 10a). On Rh/Al–Ce catalyst there existed an intermediate concentration level for N_2O, after which the concentration reached the final value. No overshooting was observed. A maximum N_2O concentration was always observed at the end of the steps, when the NO coverage can be expected to be the highest. When NO was preadsorbed during the $NO/(H_2 + NO)$ transient tests, the N_2O responses clearly showed an overshoot at the very beginning of the test at 200°C (Fig. 10b). The overshoot was highest for the Pt–Rh/Al–Ce catalyst. After a longer time from change, the concentrations reached nearly the same levels than at the end of the $H_2/(H_2 + NO)$ steps. At different temperatures the N_2O concentration levels varied according to the catalyst compositions. The correlation between the changes of the NO conversion and the N_2O formation at different temperatures is demonstrated in Fig. 11. The steady state (after 120 s

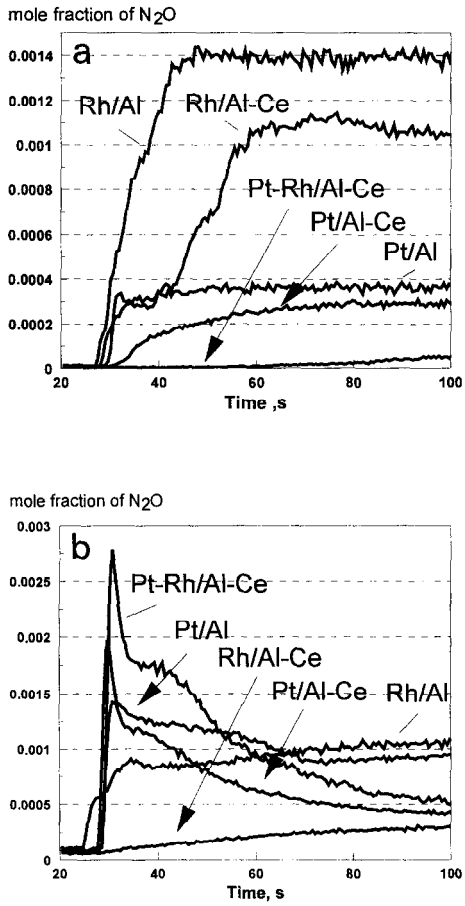

Fig. 10. The formation of N_2O in the $H_2/(H_2+NO)$ (a) and $NO/(H_2+NO)$ (b) experiments on the Pt and Rh catalysts at 200°C.

from feed exchange) NO conversion was the highest coexistent with the highest N_2O formation rates. Also, the step responses proved the inhibitory effects of NO on hydrogen adsorption. In addition of the noble metal–ceria interactions, the cooperative performance of platinum and rhodium was evident in these transient tests, because the adsorption and reaction responses cannot be understood solely as a cumulative effect from the properties of platinum and rhodium on the promoted alumina support (Figs. 2, 10 and 11). The remarkable difference between the responses of $NO/(H_2+NO)$ and $H_2/(H_2+NO)$ over Pt–Rh/Al–Ce noticed at 200°C can be explained by the state of rhodium. In the former step Rh is assumed to be mainly as Rh_2O_3, but in the latter step as metallic Rh at the beginning of the step. This fact changes the prevailing cooperative mechanism between platinum and rhodium in transient phases, where the composition of mixture fluctuates between rich and lean conditions.

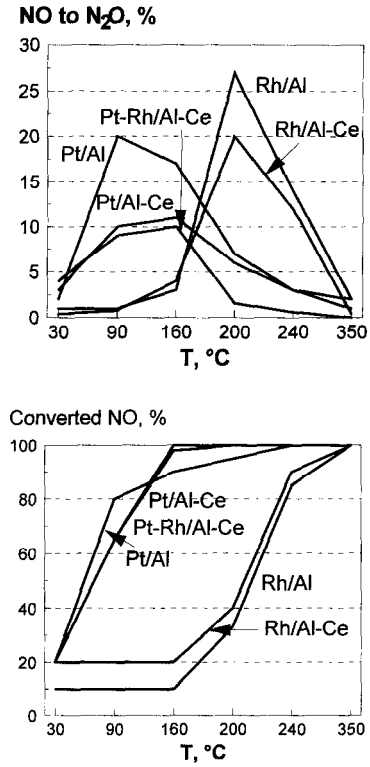

Fig. 11. The correlation between the NO conversion and the N_2O formation during $H_2/(H_2 + NO)$ at steady state (after 120 s).

At higher temperatures ($> 350°C$) the N_2O formation was negligible, but it does not exclude N_2O as a plausible intermediate, which however disappears, in a fast surface reaction [25]. The isolated $N_2O + CO$ reaction has also been reported to be very slow.

In the presence of a reducing agent, such as H_2 or CO, these molecules are able to pick up surface oxygen, e.g., for hydrogen we can write:

$$H^* + O^* \rightleftharpoons OH^* + * \tag{20}$$

$$OH^* + H^* \rightleftharpoons H_2O^* + * \tag{21}$$

$$H_2O^* \rightleftharpoons H_2O + * \tag{22}$$

For the CO_2 formation the process would correspond to that of CO oxidation, i.e., Eq. (8).

This kind of mechanism is very close to that proposed by Cho [22] for NO reduction and CO oxidation on Rh/Al_2O_3 catalysts. It should, however, be emphasized that the present study as such does not completely rule out the

possibility for a direct Langmuir-Hinshelwood type surface reaction between the reducing and oxidizing agents, i.e., between CO^* and NO^*

$$CO^* + NO^* \rightleftharpoons CO_2 + N^* + * \quad (23)$$

which has been proposed earlier by Banse et al. [26]. Analogously, adsorbed NO^* could react with adsorbed hydrogen giving dissociated nitrogen or a surface complex (HNO^*),

$$NO^* + H^* \rightleftharpoons N^* + OH^* \quad (24)$$

$$NO^* + H^* \rightleftharpoons HNO^* + * \quad (25)$$

which reacts with hydrogen giving adsorbed nitrogen:

$$HNO^* + H^* \rightleftharpoons H_2O^* + N^* \quad (26)$$

The catalytic cycle is then completed by nitrogen combination and water desorption steps in Eqs. (17) and (22), respectively. An analogous mechanism to (25)-(26) has been suggested by Katona and Somorjai [27] for the reduction of NO with NH_3 on Pt.

NO dissociation can thus proceed as an independent decomposition or it can be a reaction associated with hydrogen or CO. Instead of H^*, OH^* can also assist NO dissociation.

Reactions on Pt, Rh and Pt–Rh catalysts can be explained by similar reaction mechanisms but they had different rates on the surface. Pt was more active than Rh for NO reduction by hydrogen. Probably Pt is more active than Rh to dissociate hydrogen. Rh has the important role in commercial three-way catalysts, because it decreases the formation of ammonia in rich conditions and it is more active to initiate the NO–CO reaction and N_2O decomposition. Pt–Rh/Al–Ce had the same or higher activity than Pt/Al–Ce, but the former catalyst promoted some N_2O formation at very low temperatures ($< 160°C$). Schematic reaction pathways for NO reduction according to the proposed mechanism are shown Fig. 12.

The presented qualitative analysis demonstrated the significance of the competitive adsorption effect (NO and H_2) as well as nitrous oxide as a surface

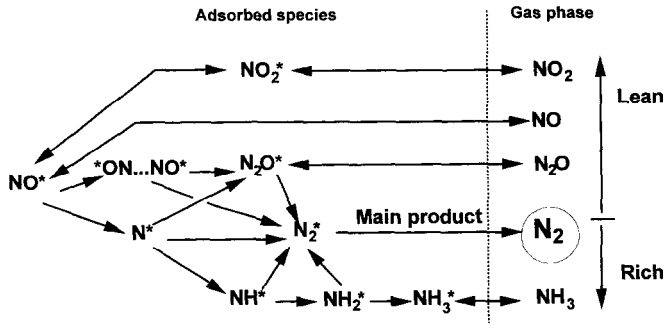

Fig. 12. The schematic reaction pathways for NO reduction.

intermediate. For a further discrimination between the surface reaction mechanisms the characterization of the surface intermediates by infrared techniques is necessary. The confirmation of the nitrogen fixation by the proposed routes becomes a main target in the future quantitative kinetic analysis. The ON...NO mechanism presented in this paper offers a plausible route for nitrogen formation without NO dissociation, which explanation is probable especially in lean conditions on metal oxide catalysts.

4. Conclusions

The oxidation of CO and the reduction of NO as well as the adsorption characteristics of CO, NO, O_2 and H_2 were studied on Pt/Al_2O_3, Rh/Al_2O_3, Pt/Al_2O_3–CeO_2, Rh/Al_2O_3–CeO_2 and Pt–Rh/Al_2O_3–CeO_2 catalysts using the transient response techniques. The experiments revealed the high adsorption capacities of the ceria promoted catalysts, which is due to the adsorbate spillover in intimate noble metal–ceria interactions. These experiments showed that close to stoichimetric mixtures, the surface coverage dynamics is reflected in small gas phase concentration deviations.

The transient response study of CO oxidation indicated that the oxidation proceeds through a bimolecular surface reaction step, between adsorbed CO and dissociated oxygen. The NO reduction studies revealed the formation of N_2 as a main product and N_2O as a by-product. The NO reduction mechanism could include the formation of N_2O through NO dissociation and active sites regeneration by reducing agents. The other possibility is a reaction assisted dissociation of NO. The fixation mechanism of nitrogen atoms was proposed for two adjacently adsorbed NO molecules. High NO coverages favored N_2O formation, but as soon as NO coverage decreased, N_2O diminished. The formation of the N–N bonding was assumed to take place totally prior to ($2N^* \rightarrow$ nitrogen), partly prior to ($N_2O^* \rightarrow$ nitrogen) or totally following to ($^*ON...NO^* \rightarrow$ nitrogen) the breakage of two N–O bondings, which is necessary to form nitrogen. NO inhibition on hydrogen adsorption and dissociation was decreased by ceria. Pt was shown to be more efficient than Rh to activate hydrogen in the NO reduction.

References

[1] K.C. Taylor, Catal. Sci.-Technol., Springer-Verlag, New York (1984) 170.
[2] I. Halasz, A. Brenner, M. Shelef, Cat. Lett., 22 (1993) 147.
[3] H. Muraki, H. Shinjon, H. Sobukawa, K. Yokota, Y. Fujitani, Ind. Eng. Chem. Prod. Res. Dev., 24 (1985) 43.
[4] C. Howitt, V. Pitchon, G. Maire, J. Catal., 154 (1995) 47.
[5] M. Shelef, G.W. Graham, Catal. Rev.-Sci. Eng., 36 (1994) 433.

[6] C.O. Bennett, in ACS Symp. Series, 178, Washington D.C., Am. Chem. Soc., (1982) 1.
[7] M. Kobayashi, Chem. Eng. Sci., 37 (1982) 393.
[8] S.-N. Wang, H. Hofmann, in Unsteady State Processes in Catalysis, Y.S. Matros (Ed.), VSP BV., Utrecht (1990) 253.
[9] M.B. Cutlip, A.I.Ch.E.J., 25 (1979) 502.
[10] Catalytica Associates Inc. (Ed.), New Catalytic Materials, Vol. XI, Montain View (1984).
[11] J.L. Falconer, J.A. Schwarz, Catal. Rev.-Sci Eng., 25 (1983) 141.
[12] T. Salmi, Chem. Eng. Sci., 43 (1988) 503.
[13] C. Serre, F. Garin, G. Belot, G. Maire, J. Catal., 141 (1993) 1.
[14] R.L. Keiski, M. Härkönen, A. Lahti, T. Maunula, A. Savimäki, T. Slotte, Stud. Surf. Sci. Catal., 94 (1995) 85.
[15] S.H. Oh, G.B. Fisher, J.E. Carpenter, D.W. Goodman, J. Catal., 100 (1986) 360.
[16] C. Serre, F. Garin, G. Belot, G. Maire, J. Catal., 141 (1993) 9.
[17] R.K. Herz, Ind. Eng. Chem. Prod. Res. Dev., 20 (1981) 451.
[18] N.I. Il'chenko, Russ. Chem. Rev., 41 (1972) 47.
[19] M. Huuska, T. Maunula, Proc. 10th Int. Cat. Congress, Budapest (1992).
[20] C.J. Casewit, A.K. Rappe, J. Catal., 89 (1984) 250.
[21] R.W. McCabe, C. Wong, J. Catal., 121 (1990) 422.
[22] B.K. Cho, J. Catal., 115 (1989), 486.
[23] J.L. Glad, V.N. Korchak, Surf. Sci., 75 (1978) 333.
[24] B. Subramaniam, A. Varma, Chem. Eng. Commun., 21 (1983) 221.
[25] B.K. Cho, J. Catal., 148 (1994) 697.
[26] B.A. Banse, D.T. Wickham, B.E. Koel, J. Catal., 119 (1989) 238.
[27] T. Katona, G.A. Somorjai, J. Phys. Chem., 96 (1992) 5465.